VACUUM ARC DEPOSITION AND CORROSION BEHAVIOUR OF PATTERNED AND COLOURED TiN/TiO_2 COATINGS ON GLASS

AV Kazakevich[1], OV Gribkova[1], BB Straumal[2,3], NF Vershinin[2], B Baretzky[3], W Gust[3], A Sánchez Bolinches[4]

[1]Moscow Institute of Steel and Alloys (Technical University), Leninsky Prosp. 4, 117049 Moscow, Russia

[2]I.V.T. Ltd. (Institute for Vacuum Technology), P.O. Box 47, 109180 Moscow, Russia

[3]Institut für Metallkunde and MPI Metallforschung, Seestr. 92, D-70174 Stuttgart, Germany

[4]Departamento de Ingeniería Mecánica y de Materiales, Universidad Politécnica de Valencia, Camino de Vera, s/n, 46022 Valencia, Spain

ABSTRACT

An industrial installation for vacuum arc deposition is presented. Its potential in the field of decorative coatings for large area glass sheets is demonstrated. Particularly it is possible to deposit naturally and interferentionnally coated as well as patterned coatings. The possibility to deposit uniform multilayer coatings having various interference colors onto large silica glass sheets is shown. Titanium nitride, titanium dioxide and bilayer TiN/TiO_2 coatings on silicate glass have been characterized in terms of composition and corrosion resistance. The depth profiling was made with the aid of Auger electron spectroscopy. The morphology and microstructure of the coatings were studied with the aid of scanning electron microscopy. The athmospheric corrosion was studied and electrochemical tests of vacuum arc deposited Ti, TiN and TiO_2 coatings in different solutions at various pH values were performed. The corrosion resistance of TiN coatings is higher than that of TiO_2. The corrosion resistance of vacuum arc deposited TiN coatings on glass proves to be higher than that of TiN coatings produced by direct current reactive sputtering and plasma assisted chemical vapour deposition. Mask-deposited TiN coatings do not show any signs of an accelerated corrosion along the border between the coated and uncoated glass.

INTRODUCTION

In modern archtitecture the conventional glass is progressively substituted by special glasses which are tempered and/or coated with layers improving the functional or decorative properties of glass [1, 2]. Recently, the vacuum arc technology was applied for the deposition of coatings on the large area glass substrates [3]. This technology was successfully used since 1970s for the deposition of hard and wear resistant coatings on cutting tools, medical equipment and heads of videorecorders [4]. The intrinsic advantages of the vacuum arc deposition permit to deposite easily the coatings on nonconducting substrates. A rather weak dependence of the deposition rate both on the distance between the target and substrate and their mutual orientation [5] allows one, on the one hand, to control precisely the thickness of the coating on large area substrates and, on the other hand, to coat effectively three-dimesional parts of complicated form. The substrate temperature during the vacuum arc deposition is very low. Therefore, is is possible to coat the polymeric parts which are sensitive to heating and to use the polymeric masks in order to produce the patterned coatings [3]. The coated architectural and automotive glasses are exposed to the detrimental influence of the enviromennt and have to be corrosion resistant. Therefore, this paper is devoted to the investigation of the corrosion resistance of silicate glasses vacuum arc coated with Ti, TiN and TiO_2.

EXPERIMENTAL

The "Nikolay" industrial scale system used for the deposition of coatings on large area architectural glasses has the following characteristics: size - 6000×3000×3000 mm, mass - 15500 kg, maximum power consumed - 75 kW, ultimate vacuum - 5×10^{-4} Pa, maximum size of treated glass - 2100×1300×8 mm, output capacity - 30 glass 2100×1300×5 mm sheets in a 8 h cycle, up to 1000 m^2/month. The standard procedure for glass decorative coating includes three steps. The glass sheet before being loaded into the machine was precleaned using hot distilled water. Afterwards, the glass sheets were mounted on metallic frames and placed in the vacuum chamber. Each frame contained two glass sheets, mounted back to back. The frame were inserted into a slot (15 slots are available) and allowed to move independently inside the machine. The displacement velocity of the frame was monitored and controlled. Each pair of glass sheets was sputter cleaned immediately before coating

using a large aperture (1400 mm in the vertical direction) Hall current accelerator [6]. The gas ionization and the subsequent ion acceleration is made through the presence of crossed electric and magnetic fields. Sheets to be treated are successively transported under the Hall discharge accelerator at a given translation speed, the substrate surface being perpendicular to the ionic flux axis. Changing the speed and accelerator power, one can control the sputter dose received by the substrate. Two Hall current accelerators are mounted in the machine. They are placed on both sides of the machine in order to clean the two sheets of the frame simultaneously. For Ar the sputter voltage is typically 5 kV, and the sputter current can vary from 1 to 6 A. Three sources with flat round targets with diameter of 200 mm are placed on each side of the installation. The surfaces of the targets are parallel to the glass substrates. Only two sources are normally used during the deposition. Arc voltage is constant at U = 22 V while the discharge current I on each source can be varied from 100 to 300 A. No bias was applied to the substrate. A reactive gas (oxygen or nitrogen) is introduced at a pressure of 0.05 Pa if an oxide or nitride coating is to be formed. The arc generation is continuous and random. The arc sources are positioned on a rather big distance (about 800 mm) from the sheets to be coated. The configuration of the machine provides shielding and increases the charged particle part of the beam using the fact that the microdroplets are ejected at small angles with respect to the target surface [7]. The distance of the glass sheet from the traget depends on the position of the frame. Therefore, the thickness of the deposited layer was controlled by varying the translation speed of the frame. The translation speed vary from 0.5 to 3 m/min in dependence on the thickness of the coating (typically 300 to 500 nm). When decorative patterns have to be produced, light nylon patterned sheets were used to provide masking. Various colours can be produced depending on the gas and deposition parameters used. In this study Ti, TiN and TiO_2 coated silicate glass samples were cut from large glass sheets and the surface morphology, composition and corrosion resistance were analysed.

The microstructure of the TiN and TiO_2 coatings was studied using scanning electron microscopy (SEM) using the JEOL JSM-6300F with an electron beam microanalysis facility. The composition depth profile of TiN/TiO_2 coated silicate glass was performed by Auger electron spectroscopy (AES) on a Physical Electronics PHI-551 spectrometer with a double-pass cylindrical mirror analyzer. The analysis was carried out with the excitation beam normal to the specimens. The spectra were taken during argon ion sputtering which produced a relatively clean surface of the sample under study without baking the system. The etching rate was considerably faster than the adsorption rate of the active residual gases. The base pressure was less than 2×10^{-8} Pa. The spectra were excited by an electron beam with an energy of 3 keV and a current of 8 μA to the sample. The peak-to-peak modulation was 3V. The sputtering was accomplished using a 5 keV Ar^+ ion beam. An ion gun was mounted to give a beam incidence angle of 70^o, and in order to minimize possible crater effects, it was rastered. The pressure of argon during sputtering was 3×10^{-3} Pa. The sputter rates for SiO_2 were determined to be 25 nm/min. Auger studies of the Ti–N system are complicated by the fact that the main Auger $KL_{2,3}L_{2,3}$ transition for nitrogen (379 eV) overlaps the titanium $L_3M_{2,3}M_{2,3}$ transition (383 eV) to produce a single peak at 381 eV [8]. Auger spectra of titanium nitride coating hence include two peaks, the one corresponding to the Ti $L_3M_{2,3}M_{4,5}$ transition (418 eV) and a TiN peak resulting from overlapping (385 eV). For quantitative analysis, one must be able to resolve the nitrogen peak by removing the titanium contribution to the 385 eV peak. This was performed using the method described previously [9] where the approach [8] was improved. The reflectivity R of coloured coatings were measured with standard lock-in techniques. White light from a halogen lamp was focussed on the entrance slit of a monochromator and the monochromatic light was focussed onto a silicon diode after reflecting on the sample.

The corrosion behaviour of Ti, TiN and TiO_2 coatings on silicate glass was characterized. The standard accelerated tests on atmospheric corrosion were carried out according to the Russian standards RST 9.012, 9.017 and 9.020 (temperature 22–25°C, humidity 96–98%, no water condensation, under influence of gaseous chlorides, NH_3 and SO_2). Accelerated tests in 3.5% NaCl solution at 22–25 °C under both full and partial immersion were also carried out. Both uniform and mask-deposited TiN coatings were studied because on the boarder between coated and uncoated glass the TiN/glass interface is exposed to the corrosion medium. The polarization behaviour was measured potentiodynamically with the aid of a potentiostatic apparatus PI-50-1/PR8 of MSNP. All potential values are given versus an Ag/AgCl electrode ($E_{Ag/AgCl}$ = 0 corresponds to – 200 mV on the hydrogen electrode scale). The scanning rate was 1 mVs^{-1}. The polarization was changed from – 0.8 V to + 1.5 V. Before the potentiodynamic measurements, the corrosion potential E_c was monitored for 0.5 h. The measurements were carried out in the electrolytes of 3.0% NaCl solution with pH = 4, 6 and 8 and 3.0 % NaCl + 3.0 % NH_4Cl solution with pH = 2, 4 and 6. The pH value of the solutions was corrected by adding of 0.05 mole of NH_4OH to the solutions containing NH_4Cl and by adding of 0.05 mole of NaOH to the solutions without

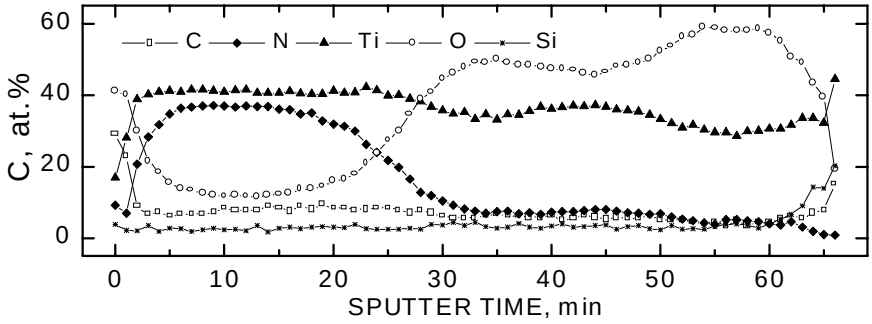

Fig. 1 AES depth profile for TiN/TiO_2 bilayer coating on the silicate glass

NH_4Cl. The pH value of the solution was controlled by a "pH-121" pH-meter of MSNP. The solution was prepared from reagent-grade chemicals and distilled water. The area exposed to the solution was 1 cm^2, the reminding surface of the samples was isolated by a varnish layer. The test temperature was 22–25 °C.

RESULTS AND DISCUSSION

Vacuum arc deposition produced architectural glass (with standard dimensions of 1300×1600 mm) has the following coatings:

(1) Thin semitransparent TiN coatings for glazing or thick nontransparent for mirrors. The colour of these coatings was determined mainly by the composition of TiN.
(2) TiO_2 coatings having interferencial colours defined by the thickness of the coating. TiO_2 coatings of two different thicknesses were characterized (green and red).
(3) Thin non transparent Ti coatings for mirrors.
(4) TiN patterned coatings. In this case the light polymeric mask was positioned between the vacuum arc source and the substrate. An example of a mask deposited coating is shown in [3]. The natural colour TiN coating was combined with uncoated transparent glass.
(5)

The depth concentration profile obtained from the Auger spectra is shown in Figure 1 for the TiN/TiO_2 bilayer coating on silicate glass. The peak characteristics for titanium, oxygen, nitrogen, carbon and silicon were analyzed. After about 3 min of sputtering, the surface contamination of carbon and oxygen disappear from the spectra. After that, the oxygen content remains unchanged in the TiN layer and the carbon concentration is nearly constant in the whole coating (slightly below 10 at.%). Quantitative analysis reveals that the Ti to N ratio in the TiN layer is about 1.1. After about 25 min of sputtering, the transition from the TiN to TiO_2 layer can be clearly seen. The titanium content is roughly uniform along the depth of the coating. The increasing concentration of silicon marks the transition from the coating to substrate. At the coating/substrate interface, nitrogen is virtually absent and the oxygen content climbs up to 60 at.% as the titanium content slightly falls down to 30 at.%. The stability of the composition of the TiN layer which does not change significantly with depth is comparable with that of TiN coatings obtained with the aid of the CVD technique [10]. Regarding composition, our TiN samples are similar to those ones obtained by the aid of plasma-assisted chemical vapor depostion (PACVD) deposited at 430°C substrate temperature, 60 W radio frequency power presented in [11]. In [11] the stoichiometric composition was obtained for substrate temperatures above 500°C. In our case the substrate temperature is well below 100°C which allows one to use polymer masks for the deposition of patterned TiN and TiO_2 coatings. It was shown [12] that even a rather high residual carbon content does not affect drastically the properties of TiO_2. In our case, the high corrosion resistance of the vacuum arc deposited coatings also reveals that the carbon contamination is not critical.

In Figures 2 to 5 the SEM micrographs of Ti, TiN and TiO_2 coatings both intact (Fig. 3) and after 15 min corrosion in NaCl solution (pH=4) at various implied voltages *E* are presented. The most important structural feature of both TiN and TiO_2 coatings are the Ti microdroplets present in the coating [5]. The droplets have various dimensions (in comparison with the thickness of the deposited film) and meet the substrate at various time during the deposition process. In dependence on the ratio (droplet thickness/coating thickness) and the time the following morphologically different situations case can be defined (Figure 6): (1) The droplet formed early in the deposition process and contacts immediately the substrate, but is completely buried in the film; (2) The

Fig. 2 Vacuum arc deposited coatings after corrosion test in NaCl (E_c = + 0.3 V, pH = 4, 15 min). (a) Ti, (b) TiN, (c) TiO_2

Fig. 3 Intact vacuum arc deposited coatings before corrosion test. (a) Ti, (b) TiN, (c) TiO_2

Fig. 4 Vacuum arc deposited coatings after corrosion test in NaCl (E_c = – 0.3 V, pH = 4, 15 min). (a) Ti, (b) TiN, (c) TiO_2

Fig. 5 Vacuum arc deposited coatings after corrosion test in NaCl (E_c = – 0.7 V, pH = 4, 15 min). (a) Ti, (b) TiN, (c) TiO_2

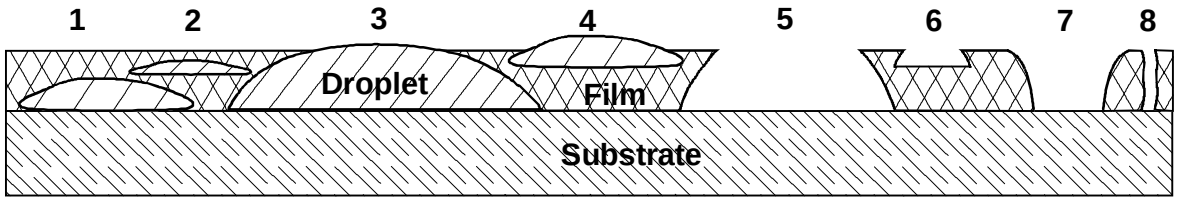

Fig. 6 The morphology of the microdroplets in a vacuum arc deposited film (see text)

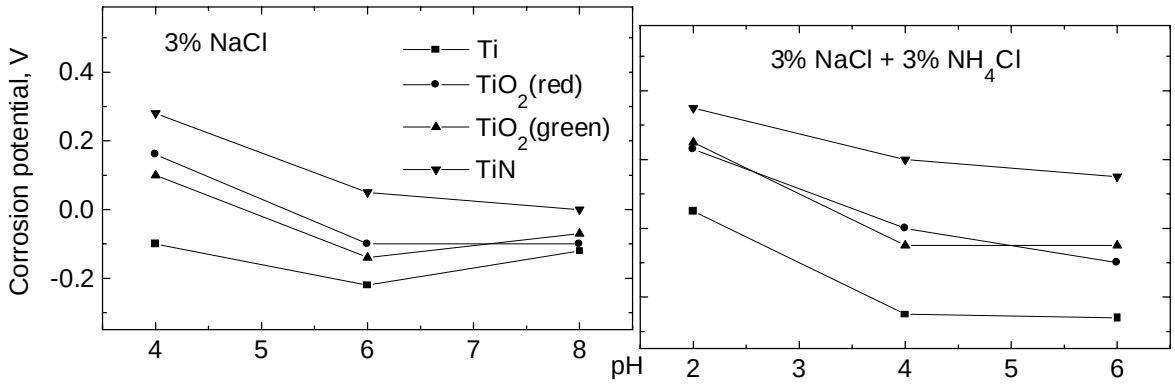

Fig. 7 The corrosion potentials of the Ti, TiN and TiO_2 coatings studied

droplet later is completely buried and has the film material both below and above; (3) The big droplet contacts the substrate and is not completely buried; (4) A small droplet has no contact with the substrate and is not completely buried; (5) A small droplet is fallen apart during or after coating, the coating is thinner in this location but no substrate is visible, (6) large dropled is fallen apart during or after coating, the coating is absent in this location, the substrate is exposed. Pin-holes penetrating the coating (7) can also be present. If we deal with decorative coating deposited through the mask, the coating is completely absent in some locations shutted by the mask (8) and the substrate is exposed to the atmosphere and corrosion agents. From the point of view of corrosion, the metallic droplets in the coating may be deteriorative. However, the metallic droplets in the nitride or oxide coatings form the interface which can be easier attacked by the corrosion agents, especially in the cases like (3) or (6). The microdroplets are so small that they are not visible to a naked eye. They do not disturb the appearance of coated glasses and, therefore, they do not restrict their applicability as architectural materials. Nevertheless, in case of a less corrosion resistant substrate (stainless steel instead of glass), the small pores surrounding these droplets can feed the corrosive agent to the substrate, and active corrosion starts. Visual examination of Ti, TiN and TiO_2 coatings before and after electrochemical corrosion testing in a neutral solution revealed differences in the corrosion mechanism. It can be seen in Fig. 3 where the coatings deposited under similar conditions are shown that the number of Ti droplets is minimal in TiN coatings and maximal in the TiO_2 coatings. This feature is defined by the different mechanisms of the interaction between Ti ions and oxigen or nitrogen during the formation of nitride or oxide. The corrosion of TiO_2 coatings started at low E values (both positive and negative) and formed dark corroded regions around the Ti microparticles. The number and area of corroded places uniformly increased with increasing E (Figs. 2c, 4c and 5c). The corrosion of Ti coatings proceeds also iniformly (Figs. 2a, 4a, 5a), and the local delaminations and bubbles are clearly visible (Fig. 5a). The TiN coatings were stable against corrosion and did not reveal any visual signs of damage (Fig. 2 b, 5b) up to rather high positive and negative E values (– 0.8 V and + 0.7 V). Above E = + 0.7 V, multiple corroded areas suddenly appeared all over the surface, destroying the coating almost simultaneously everywhere (Fig. 5b). After 12 months of exposure to atmospheric corrosion with conditions which correspond to the most aggressive type of the industrial atmosphere (temperature 22–25°C, humidity 96–98%, no water condensation, under influence of gaseous chlorides, NH_3 and SO_2), neither the mass nor appearance changed. Likewise, neither full nor partial immersion in NaCl solution for 8 months produced any changes. The first signs of corrosion in these tests appeared only after 11 months. This high corrosion resistance is comparable with the properties of vacuum arc deposited TiN coatings on steel and brass substrates [13]. The mask-deposited TiN coatings did not show any signs of accelerated corrosion along the border between coated and uncoated glass.

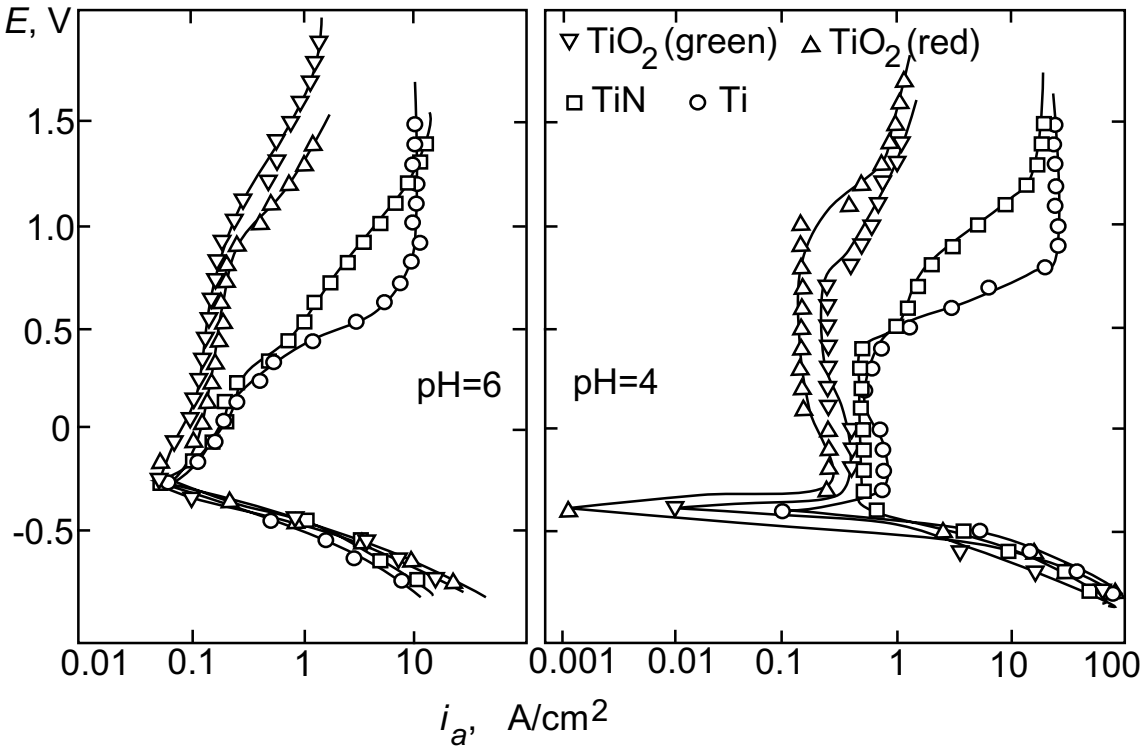

Fig. 8 The dependence of the corrosion current i_c on the polarisation voltage E in a 3.0 at.% NaCl solution with pH = 4 and pH=6

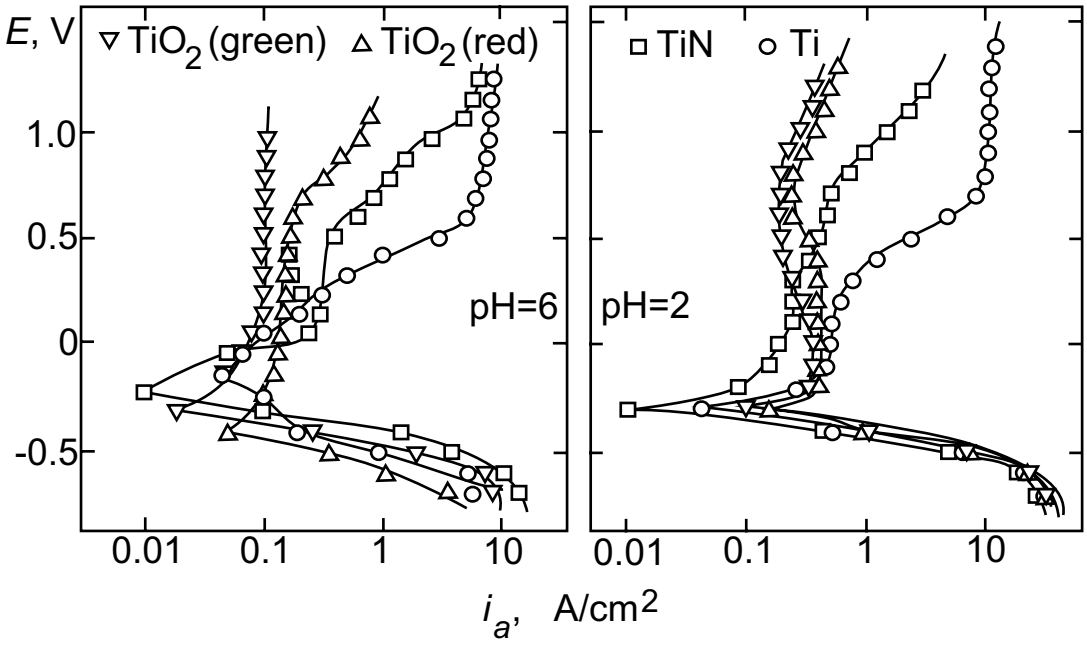

Fig. 9 The dependence of the corrosion current i_c on the polarisation voltage E in a 3.0 at.% NaCl + 3.0 at. % NH_4Cl solution with pH=2 and pH=6

The data of electrochemical tests are displayed in Fig. 6 (NaCl solution, pH = 4 and pH = 6) and Fig. 7 (NaCl + NH_4Cl solution, pH = 2 and pH=6). The dependence of the corrosion current i_c on the polarisation voltage E is shown for Ti, TiN and two different TiO_2 coatings of various thickness having red and green colours. Both TiN and TiO_2 were self-passivated. The corrosion potentials are given in Fig. 7. This data show that at a low pH value, the corrosion resistance of TiN is much higher than that of Ti and TiO_2 in both solutions studied. Furthermore, the TiO_2 coating is more corrosion resistant than pure Ti. With increasing pH, E_c becomes more negative. Nevertheless, E_c in all cases remains more positive than the reduction potential for hydrogen. This indicates that the corrosion process for all coatings studied can proceed only with oxygen depolarization. The most negative E_c was measured for the Ti coatings, the most positive for TiN. It can be seen in Figs. 8 and 9 that both the cathodic and anodic processes are less pronounced on the surface of TiO_2 in comparison with TiN. The corrosion current i_a for TiN is smaller in the NH_4Cl-containing solution. The values of i_a for Ti and TiO_2 remain on the same levels as those in NaCl solution without NH_4Cl. It is also important to mention that i_a oscillates at the voltages of anodic polarization for TiO_2. This reveals that the coating surface layer is repeatedly attacked and activated. The corrosion properties of a system containing a substrate and a coating depend strongly on the electrochemical properties of both components. Numerous papers report data on the electrochemical properties of TiN deposited on metallic substrates like tool steel [11, 13–18]. The corrosion process of TiN/steel is rather complicated and includes, together with corrosion of TiN, the corrosion of the steel substrate. It can be controlled by the penetration of the corrosion agents both along the interface between the coating and substrate and through defects in the coating. To correctly discuss our results, we compare our data with the electrochemical properties of TiN deposited on electrochemically inert substrates (glass, Al_2O_3) by reactive direct current sputtering and PACVD [14, 17]. The values of corrosion current density, i_c [14, 17] are of the same order of magnitude as in this work. The corrosion potential E_c of TiN in a NaCl solution with pH = 6 in our work is about 0.09 mV more positive than E_c for nearly the same electrochemical conditions after results of [18]. For pH = 1 [14], E_c = – 0.23 V for sputtered films (recalculated for the Ag/AgCl electrode) and for pH = 12, E_c = – 0.33 V, which is much lower than both values obtained in this work. A pronounced anodic peak was present in all potentiodynamic curves [17]. In our work the coatings were self-passivated. Therefore, the corrosion resistance of TiN deposited by the vacuum arc process is definitely higher than that of TiN coatings deposited on silicate glass substrates by reactive direct current sputtering [17] and on Al_2O_3 substrates by plasma-assisted chemical vapor deposition [14].

ACKNOWLEDGEMENTS

The financial support of the Copernicus Network (contract ERB IC15 CT98 0812), the Royal Swedish Academy of Sciences, the Russian Federal Education Ministry, and the INTAS programme (contract 99-1216) is acknowledged.

REFERENCES

[1] Samyn P, Achten M, J. Non-Crystalline Solids 218 (1997) 1
[2] Arnaud A, J. Non-Crystalline Solids 218 (1997) 12
[3] Straumal B, Vershinin N, Filonov K, Dimitriou R, Gust W, Thin Solid Films 351 (1999) 204
[4] Boxman RL, Martin PJ, Sanders DM (eds.), 'Handbook of Vacuum Arc Science and Technology', Noyes Publications (Park Ridge, NJ) 1995
[5] Vershinin N, Straumal B, Gust W, J. Vac. Sci. Technol. A 14 (1996) 3252
[6] Vershinin N, Straumal B, Filonov K, Dimitriou R, Gust W, Benmalek M, Thin Solid Films 351 (1999) 172
[7] Daadler JE, J. Phys. D 9 (1976) 2379
[8] Dawson PT, Tzatzov KK, Surf. Sci. 149 (1985) 105
[9] Shulga JuM, Khodan AN, Phys. Chem. Mech. Surf. 5 (1989) 116 (in Russian)
[10] Kim DW, Park YJ, Lee JG, Chun JS, Thin Solid Films 165 (1988) 149
[11] In B, Kim SP, Kim YI, Kim WW, Kuk IH, Chun SS, Lee WJ, J. Nucl. Mat. 211 (1994) 223
[12] Babelon P, Dequiedt AS, Mostéfa-Sba H, Bourgeois S, Sibillot P, Sacilotti M, Thin Solid Films 322 (1998) 63
[13] Vershina AK, Bel'chin IA, Pitel'ko AA, Izotova SD, Fiz. Chim. Obr. Mat. No. 5 (1990) 93 (in Russian)
[14] Lunarska E, Michalsky J, J. Mat. Sci. 30 (1995) 4125
[15] Brandl W, Gendig C, Thin Solid Films 290–291 (1996) 343
[16] In CB, Kim SP, Chun JS, J. Mat. Sci. 29 (1994) 1818
[17] Massiani Y, Medjahed A, Gravier P, Argème L, Fedrizzi L, Thin Solid Films 191 (1990) 305
[18] Lunarska E, Al Ghanem S, phys. stat. sol. (a) 145 (1994) 587